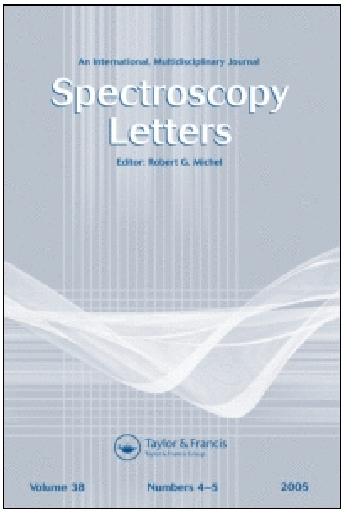

Spectroscopy Letters
Publication details, including instructions for authors and subscription information:
http://www.informaworld.com/smpp/title~content=t713597299

ANALYSIS OF THE FREQUENCY SHIFTS CLOSE TO THE SECOND ORDER PHASE TRANSITION IN NH_4Cl

H. Yurtseven[a]; D. Kayişoğlu[a]
[a] Department of Physics, Istanbul Technical University, Istanbul, Turkey

To cite this Article Yurtseven, H. and Kayişoğlu, D.(2001) 'ANALYSIS OF THE FREQUENCY SHIFTS CLOSE TO THE SECOND ORDER PHASE TRANSITION IN NH_4Cl', Spectroscopy Letters, 34: 2, 147 — 157
To link to this Article: DOI: 10.1081/SL-100002004
URL: http://dx.doi.org/10.1081/SL-100002004

SPECTROSCOPY LETTERS, 34(2), 147–157 (2001)

ANALYSIS OF THE FREQUENCY SHIFTS CLOSE TO THE SECOND ORDER PHASE TRANSITION IN NH_4Cl

H. Yurtseven and D. Kayişoğlu

Department of Physics, Istanbul Technical University,
Maslak, Istanbul, Turkey

ABSTRACT

In this study we analyzed observed Raman data for the frequencies of the disorder-induced modes of ν_7 (93 cm^{-1}) and ν_5 (144 cm^{-1}) in the second order phase region of NH_4Cl ($P = 2.8$ kbar). By means of a power-law formula describing the critical behaviour of the frequency shifts $\frac{1}{\nu}(\frac{\partial\nu}{\partial T})_p$ for those phonon modes studied, we extract the critical exponent value of $a = 0.25$, which can also describe the critical behaviour of the specific heat C_p close to the second order phase transition in NH_4Cl. Within this content, our spectroscopically modified Pippard relations are introduced here.

Key Words: Raman; Phase transition; NH_4Cl; Disorder-induced modes; Ammonium halides; Phase transitions.

INTRODUCTION

Ammonium halides have been studied extensively in the literature since they show λ type of phase transitions. In particular, the NH_4Cl crystal has been studied due to the fact that it undergoes the first order phase transition at zero pressure, the tricritical transition at ~1.6 kbar and the second order transition at ~2.8 kbar pressures. Experimentally, these phase transitions have been observed by means of the length-change measurements [1].

During those phase transformations, the crystal structures of the phases change with their symmetries. At higher temperatures the disordered β phase of ammonium halides (NH_4Cl and NH_4Br) has the CsCl structure with O_h^1 symmetry (space group Pm3m), where the NH_4^+ tetrahedra are randomly distributed between two energetically equivalent states. At lower temperatures, the CsCl structure of the β phase transforms into the tetragonal structure of the antiferro-ordered γ phase with the D_{4h}^7 symmetry (space group P4/nmm), which occurs in NH_4Br only. In the γ phase the NH_4^+ tetrahedra have the antiparallel arrangement in the a-b plane and they are parallel along the c-axis. As the temperature decreases further, the antiferro-ordered γ phase transforms into the ferro-ordered δ phase where all the NH_4^+ ions are parallel to each other (NH_4Cl and NH_4Br). The crystal structure of the δ phase is cubic with T_d^1 symmetry (space group P43m). The phase transition from the disordered β phase the ferro-ordered δ phase takes place at $T \cong 243$ K ($P = 0$) in NH_4Cl. This β-δ transition occurs at $T_C = 257$ K as the tricritical ($P = 1.6$ kbar) and at $T = 267$ K as the second order ($P \cong 2.8$ kbar) transition for the NH_4Cl crystal. Regarding the tricritical points (TCP) in the ammonium (deutero-ammonium) chloride and bromide structures, a generalized P-T phase diagram has been given by Leung et al. [2]. An experimental P-T phase diagram in ammonium halides was first obtained by Stevenson [3]. This phase diagram has been modified by Press et al. [4]. Using the Raman spectroscopic technique, the P-T phase diagrams for ammonium halides have been obtained by Ebisuzaki [5] and also by Hochheimer et al. [6]. The experimentral T-x phase diagrams in the ammonium halides have also been reported in the literature. For the $NH_4Br_xCl_{1-x}$ system the T-x phase diagrams have been obtained experimentally by Jahn and Neumann [7], Goto et al. [8], Garland et al. [9] and Yoshizawa et al. [10]. The phase diagrams in the ammonium halides have been calculated theoretically as well. Yamada et al. [11] have introduced an Ising pseudospin-phonon coupled model to predict the phase diagram of NH_4Br. Also, some other model studies due to Hüller [12], Vaks and Schneider [13], Vlasova et al. [14] have predicted the phase diagrams in the ammonium halides. Recently, we have predicted P-T phase diagrams in the ammonium halide structures using the mean field theory [15].

The λ-phase transitions in the ammonium halides, in particular, in NH_4Cl have been studied extensively. As we have given some of those studies above, the other studies have also been reported in the literature [16–24]. Among those, the Raman studies [5,19,23] have concentrated on the various aspects of the λ-phase transitions in NH_4Cl. In our early study [23] in particular, we have correlated the volume changes to the our observed Raman frequencies for the disordered-induced modes of ν_7 (93 cm^{-1}) and ν_5 (144 cm^{-1}) in the first order ($P = 0$), tricritical ($P \cong 1.6$ kbar) and second order ($P \cong 2.8$ kbar) phase regions of NH_4Cl. By using our observed Raman data, we have also calculated the specific heat C_v for those phase transitions in NH_4Cl, as given in our recent study [25].

In this study we concentrate on the temperature dependence of our observed frequencies of the disorder-induced Raman modes of $\nu_7(93\ cm^{-1})$ and ν_5 ($144\ cm^{-1}$) in the second order phase region ($P \cong 2.8$ kbar) of NH_4Cl. We analyze our Raman frequencies of those modes using a power-law formula and obtain the value of the critical exponent for the frequency shifts close to the second order phase transitions in the NH_4Cl crystalline system.

In Section 2 we give our calculations and results. Our results are discussed in Section 3. Finally, our conclusions are given in Section 4.

CALCULATIONS AND RESULTS

The λ-type of phase transitions can be studied by means of the Pippard relation in the vicinity of the λ point. The thermodynamic functions such as the specific heat C_p, thermal expansivity α_p and the isothermal compressibility κ_T, exhibit similar critical behaviour near T_λ. This critical behaviour can be expressed by means of the Pippard relations

$$C_p = \alpha_p V T \left(\frac{dP}{dT}\right)_\lambda + T \left(\frac{dS}{dT}\right)_\lambda \tag{1}$$

and

$$\alpha_p = \kappa_T \left(\frac{dP}{dT}\right)_\lambda + \frac{1}{V}\left(\frac{dV}{dT}\right)_\lambda \tag{2}$$

where $(dS/dT)_\lambda$ and $(dV/dT)_\lambda$ are constants at T_λ. Thus, linear plots of C_p versus α_p and α_p versus κ_T enable one to obtain the slope $(dP/dT)_\lambda$ in the vicinity of the λ transition point.

We have modified the Pippard relations spectroscopically by defining the isobaric mode Grüneisen parameter

$$\gamma_p = -\frac{1}{\alpha_p}\frac{1}{\nu}\left(\frac{\partial \nu}{\partial T}\right)_p \tag{3}$$

and the isothermal mode Grüneisen parameter

$$\gamma_T = -\frac{1}{\kappa_T}\frac{1}{\nu}\left(\frac{\partial \nu}{\partial P}\right)_T \tag{4}$$

as we have given in our earlier study [23]. By inserting Equations (3) and (4) into Equations (1) and (2), respectively, we then obtain our spectroscopically modified

Pippard relations given by

$$C_p = -\frac{1}{\gamma_p} T V \left(\frac{dP}{dT}\right)_\lambda \frac{1}{\nu}\left(\frac{\partial \nu}{\partial T}\right)_p + \text{constant} \tag{5}$$

and

$$\alpha_p = -\frac{1}{\gamma_T} T V \left(\frac{dP}{dT}\right)_\lambda \frac{1}{\nu}\left(\frac{\partial \nu}{\partial P}\right)_T + \text{constant} \tag{6}$$

as we have also reported in our earlier study (26). According to Equations (5) and (6), we can assume that the frequency shifts have similar critical behaviour as the specific heat C_P and the thermal expansivity α_P. Thus, we expect that the frequency shifts $\frac{1}{\nu}\left(\frac{\partial \nu}{\partial T}\right)_p$ vary linearly with the C_P (Eq. 5). We also obtain a linear variation of $\frac{1}{\nu}\left(\frac{\partial \nu}{\partial P}\right)_T$ with the α_P (Eq. 6). This critical behaviour of the frequency shifts can be expressed by a power-law formula

$$\frac{1}{\nu}\left(\frac{\partial \nu}{\partial T}\right)_p = A\varepsilon^{-a} \tag{7}$$

where **a** is the critical exponent for the frequency shifts and also for the specific heat (Eq. 5). A is the amplitude and $\varepsilon = |T - T_c|/T_c$ is the reduced temperature. By solving Equation (7) for ν, we get

$$\ln(\nu/\nu_c) = \frac{AT_c}{1-a}\,|\varepsilon|^{1-a} \tag{8}$$

where ν_c is the critical frequency at $T = T_c$. By taking the logarithm of Equation (8), we then get

$$\ln[\ln(\nu/\nu_c)] = \ln\left(\frac{AT_c}{1-a}\right) + (1-a)\ln|\varepsilon| \tag{9}$$

By plotting in the log-log scale the logarithm of $\ln(\nu/\nu_c)$ against $|\varepsilon|$, we obtain the critical exponent **a** and the amplitude A.

Similarly, we can describe the frequency shifts $\frac{1}{\nu}\left(\frac{\partial \nu}{\partial P}\right)_T$ using the power-law formula

$$\frac{1}{\nu}\left(\frac{\partial \nu}{\partial P}\right)_T = B\varepsilon^{-b} \tag{10}$$

where **b** defines the critical exponent for the frequency shifts and also for the thermal expansivity (Eq. 6) B is the amplitude and $\varepsilon = |P - P_C|/P_C$ is the reduced pressure. (P_C is the critical pressure). Similar to Equation (7), Equation (10) can also be solved for ν which gives

$$\ln(\nu/\nu_c) = \frac{BP_c}{1-b}\,|\varepsilon|^{1-b} \tag{11}$$

Here, ν_c is the critical frequency at $P = P_c$. Again, by plotting logarithm of $\ln(\nu/\nu_c)$ as a function of $\ln|\varepsilon|$, we obtain the critical exponent **b** and also the amplitude B, according to

$$\ln[\ln(\nu/\nu_c)] = \ln\left(\frac{BP_c}{1-b}\right) + (1-b)\ln|\varepsilon| \tag{12}$$

In this study we consider Equation (7) and as a result of this, Equation (9) to analyze our observed frequency data for the disorder-induced Raman modes of ν_7 (93 cm^{-1}) and ν_5 (144 cm^{-1}) in the NH_4Cl system for its second order phase transition ($P = 2.8$ kbar). For this analysis, we first calculated the critical frequencies for those phonon modes using the length-change data [1], as given in our earlier work [25].

The values of the critical frequencies for the ν_7 (93 cm^{-1}) and ν_5 (144 cm^{-1}) modes, which we obtained, were 98.16 cm^{-1} and 151.37 cm^{-1} at 266.5 K ($T < T_c$), respectively for the second order phase transition ($P = 2.8$ kbar) in the NH_4Cl [25]. Our values for those phonon modes were 95.73 cm^{-1} and 150.92 cm^{-1} at 267 K ($T > T_c$) for this phase region ($P = 2.8$ kbar) in the NH_4Cl [25].

Figures 1 and 2 give our plots of $\ln[\ln(\nu/\nu_c)]$ against $\ln|\varepsilon|$, according to Equation (9) using our observed frequency data for the ν_7 (93 cm^{-1}) Raman mode ($P = 2.8$ kbar) below and above T_c, respectively. We give those plots for the ν_5 (144 cm^{-1}) Raman mode ($P = 2.8$ kbar) below and above T_c in Figures 3 and 4, respectively. The values of **a** and A within the limits of the reduced temperature ε are tabulated for both phonon modes in Table 1.

DISCUSSION

Using our observed Raman data, the frequencies of the disorder-induced modes of ν_7 (93 cm^{-1}) and ν_5 (144 cm^{-1}) were analyzed here in the second order phase region of NH_4Cl ($P = 2.8$ kbar). By means of Equation (9) or Equation (7), from our analysis of both phonon modes, we got the same value of $a = 0.25$ for the frequency shifts above and below T_c, which can describe the second order phase transition in NH_4Cl at $P = 2.8$ kbar ($T_c = 266.6$ K). Our exponent value of $a = 0.25$ can be compared with those values of 1/16 (~0.066) for $T < T_c$ and 1/8 (0.125) for $T > T_c$ due to 3d Ising model and also 0 (discontinuous) value of the mean field theory for the specific heat. We assume here that our exponent value does not only describe the frequency shifts, but it also describes the specific heat C_p, according to Equation (5), close to the λ-phase transition in NH_4Cl. Thus, if our modified Pippard relation (Eq. 5) is satisfied close to the second order phase transition ($P = 2.8$ kbar) in NH_4Cl, the critical exponent for the frequency shifts then describes the critical behaviour of the specific heat

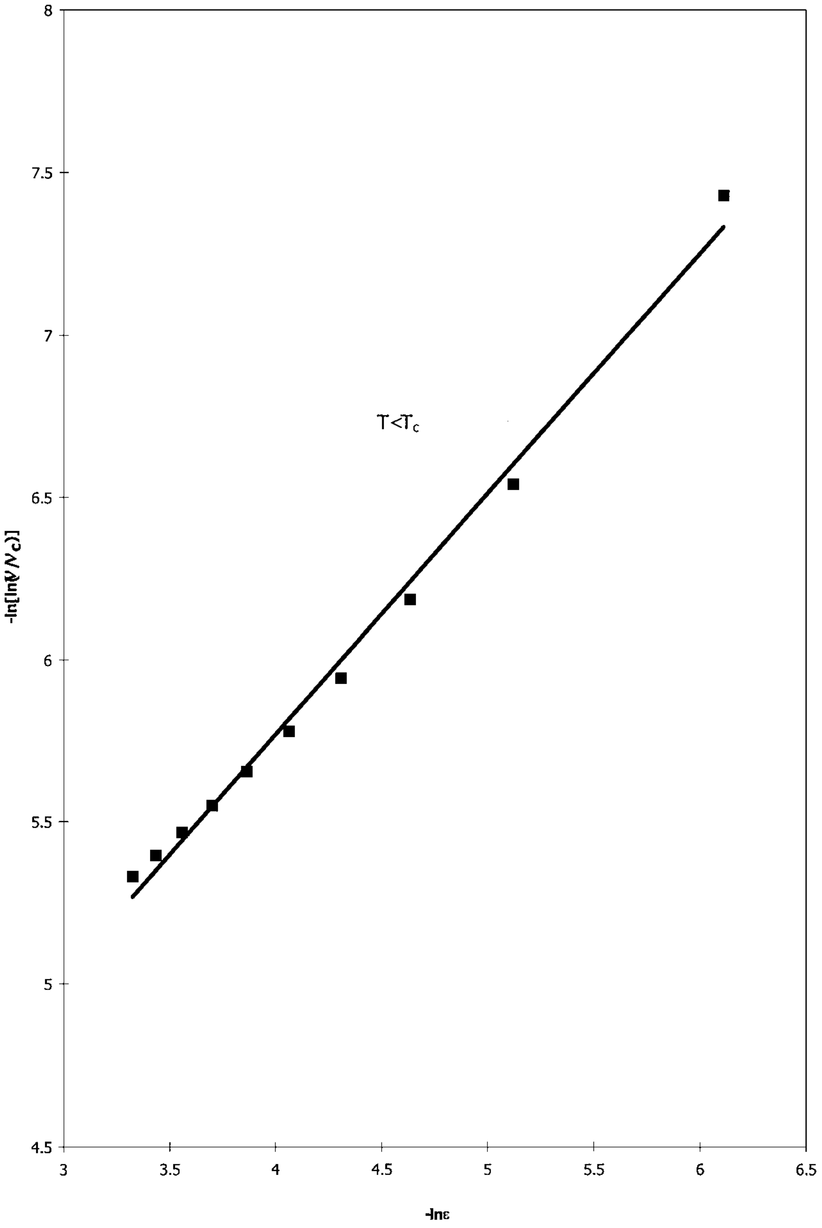

Figure 1. $\ln(\nu/\nu_c)$ for the ν_7 (93 cm^{-1}) Raman mode of NH_4Cl as a function of $\varepsilon = (T_c - T)/T_c$ for $P = 2.8$ kbar below T_c, according to Equation (9) where ν_c represents the critical frequency ($T_c = 266.6$ K). Our observed Raman data are shown by squares.

Marcel Dekker, Inc.
270 Madison Avenue, New York, New York 10016

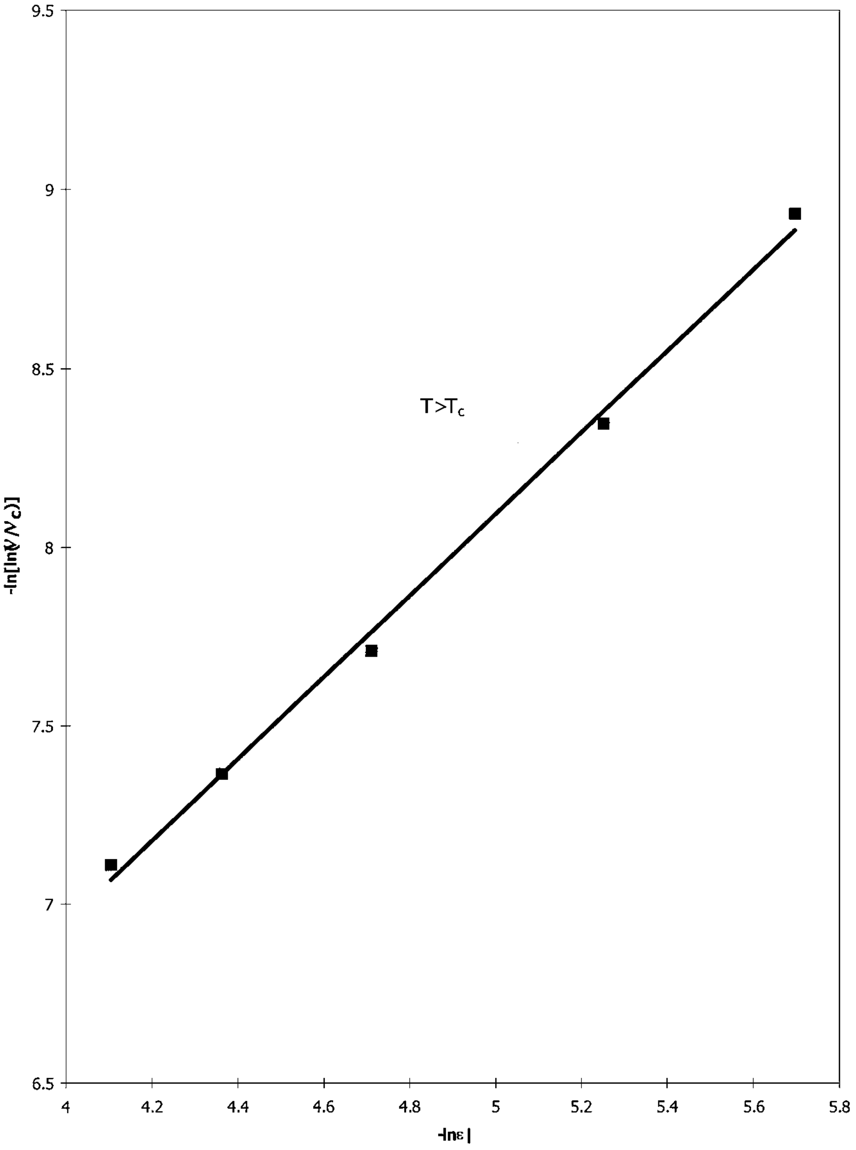

Figure 2. $\ln(\nu/\nu_c)$ for the ν_7 (93 cm^{-1}) Raman mode of NH_4Cl as a function of $\varepsilon = (T - T_c)/T_c$ for $P = 2.8$ kbar above T_c, according to Equation (9) where ν_c represents the critical frequency ($T_c = 266.6$ K). Our observed Raman data are shown by squares.

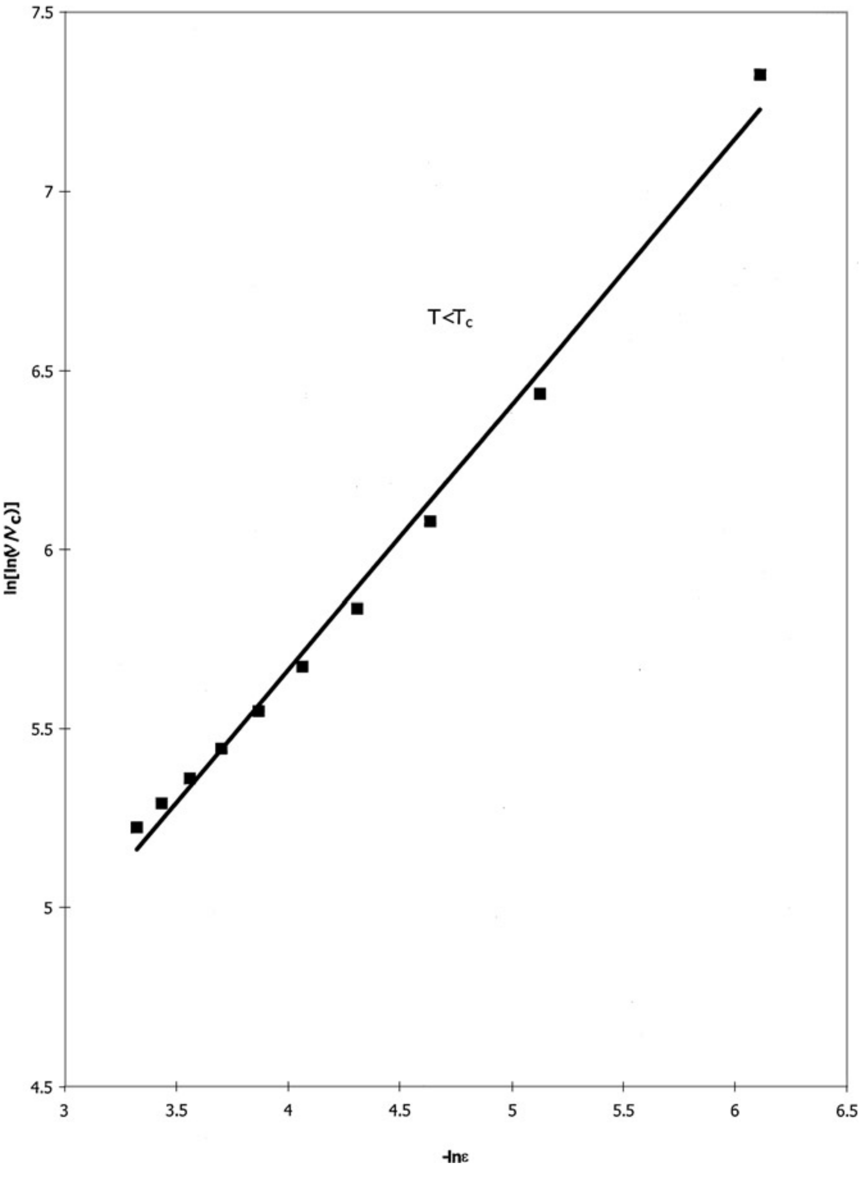

Figure 3. $\ln(\nu/\nu_c)$ for the ν_5 (144 cm^{-1}) Raman mode of NH_4Cl as a function of $\varepsilon = (T_c - T)/T_c$ for $P = 2.8$ kbar below T_c, according to Equation (9) where ν_c represents the critical frequency ($T_c = 266.6$ K). Our observed Raman data are shown by squares.

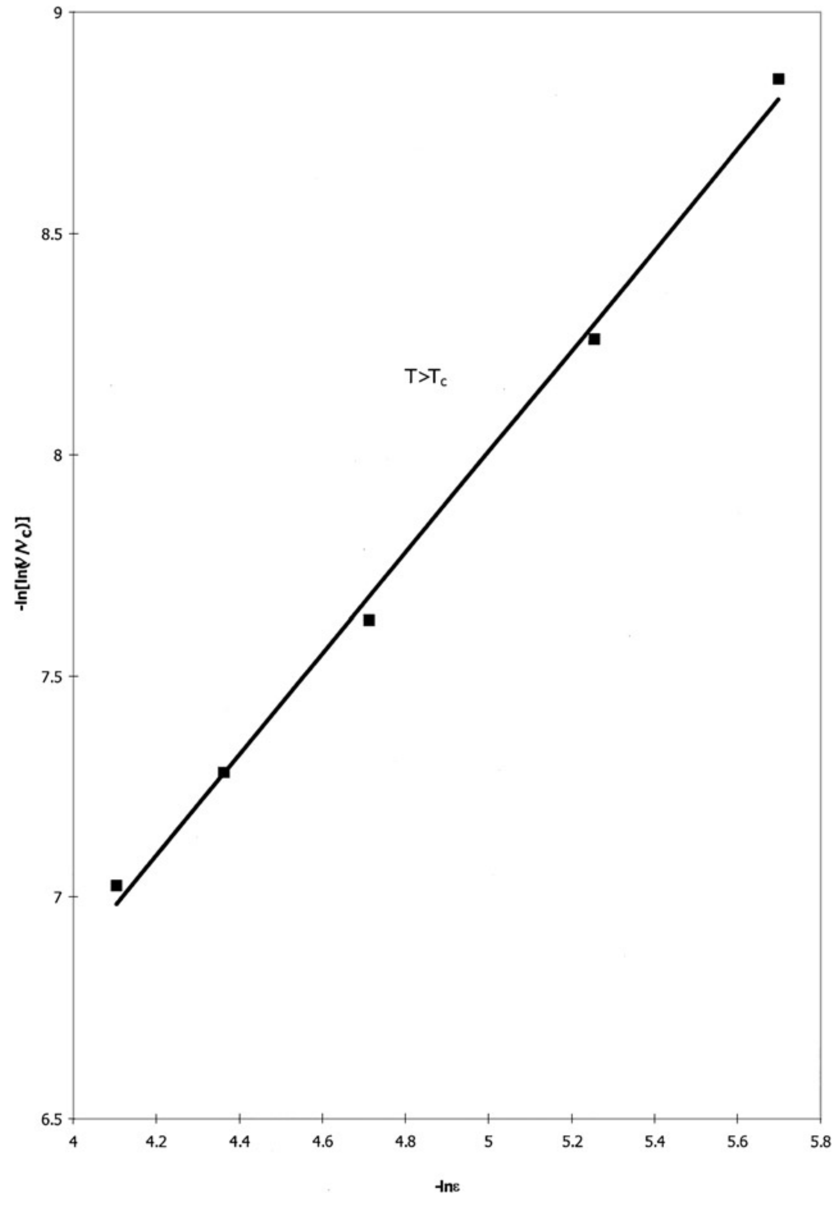

Figure 4. $\ln(\nu/\nu_c)$ for the ν_5 (144 cm^{-1}) Raman mode of NH_4Cl as a function of $\varepsilon = (T - T_c)/T_c$ for $P = 2.8$ kbar above T_c, according to Equation (9) where ν_c represents the critical frequency ($T_c = 266.6$ K). Our observed Raman data are shown by squares.

Table 1. Our Values of the Critical Exponent **a** and the Amplitude A for the Disorder-Induced Raman Modes of ν_7(93 cm^{-1}) and ν_5(144 cm^{-1}) Close to the Second Order Phase Transition ($P = 2.8$ kbar) in NH_4Cl ($T_c = 266.6$ K), According to Equation (9). The Limits of the Reduced Temperature $\varepsilon = |T - T_c|/T_c$ are Given. The Critical Frequencies of ν_7 (93 cm^{-1}) and ν_5 (144 cm^{-1}) Modes at the Temperatures Indicated Are Also Given Here

	a	A × 10^{-4} (K^{-1})	ε	T (K)	ν_c (cm^{-1})	ν_c (cm^{-1})
$T < T_c$	0.25	1.69	$2.25 \times 10^{-3} < \lvert\varepsilon\rvert < 3.6 \times 10^{-2}$	266.5	98.16	151.37
$T > T_c$	0.25	1.69	$3.4 \times 10^{-3} < \lvert\varepsilon\rvert < 1.65 \times 10^{-2}$	267	95.73	150.92

C_p. This assumes that the isobaric mode Grüneisen parameter γ_p remains constant right through the phase transitions in NH_4Cl as we also noted in our earlier studies [23,25].

Similar analysis can be carried out to determine the critical exponent **b** for the frequency shifts with the pressure at constant temperatures $\frac{1}{\nu}\left(\frac{\partial \nu}{\partial P}\right)_T$, according to Equation (10) or Equation (12), close to the second phase transition in NH_4Cl. This requires the Raman frequencies measured as a function of pressure at constant temperatures for the ν_7 (93 cm $^{-1}$) and ν_5 (144 cm $^{-1}$) modes of NH_4Cl close to the phase transitions in this crystalline system. This then leads us to examine the second Pippard relation, which we modified spectroscopically (Eq. 6) by means of the thermal expansivity data for NH_4Cl close to the phase transitions in this crystal. As for the isobaric mode Grüneisen parameter γ_p in Equation (5), we also assume that the isothermal mode Grüneisen paramter γ_T remains constant across the phase transitions in NH_4Cl for the validity of Equation (6). By means of both relations (Eqs. 5 and 6), the value of the slope $(dP/dT)_\lambda$ can be calculated close to the λ-phase transitions in NH_4Cl and they can be compared with that measured experimentally.

CONCLUSIONS

We studied here the disorder-induced Raman modes of the ν_7 (93 cm $^{-1}$) and ν_5 (144 cm^{-1}) close to the second order phase transition in NH_4Cl ($P = 2.8$ kbar). Our observed Raman data were analyzed for those phonon modes, which gave us the exponent value of $a = 0.25$ for the frequency shifts $\frac{1}{\nu}\left(\frac{\partial \nu}{\partial T}\right)_p$. We assume that our exponent value also describes the critical behaviour of the specific heat C_p, according to the validity of our spectroscopically modified Pippard relation close to the second order phase transitions in NH_4Cl. Our exponent value is close to the values of 1/8 ($T > T_c$) and 1/16 ($T < T_c$) predicted by a 3d Ising model for the specific heat.

REFERENCES

1. Weiner, B.B.; Garland, C.W. J. Chem. Phys. **1972**, *56*, 155.
2. Leung, R.C.; Zahradnik, C.; Garland, C.W. Phys. Rev. **1979**, *B19*, 2612.
3. Stevenson, R. J. Chem. Phys. **1961**, *34*, 346.
4. Press, W.; Eckert, J.; Cox, D.E.; Rotter, C.; Kamitakahara, W. Phys. Rev. **1976**, *B14*, 1983.
5. Ebisuzaki, Y. Chem. Phys. Lett. **1973**, *19*, 504.
6. Hochheimer, H.D.; Spanner, E.; Strauch, D. J. Chem. Phys. **1976**, *64*, 1583.
7. Jahn, I.R.; Neumann, E. Solid State Comm. **1973**, *12*, 721.
8. Goto, T.; Fujimura, T.; Kamiyoshi, K. Phys. Stat. Solidi (a) **1978**, *45*, 513.
9. Garland, C.W.; Leung, R.C.; Zahradnik, C. J. Chem. Phys. **1979**, *71*, 3158.
10. Yoshizawa, M.; Fujimura, T.; Goto, T. Kamiyoshi, K. J. Phys. C: Solid State Phys. **1983**, *16*, 131.
11. Yamada, Y.; Mori, M.; Noda, Y. J. Phys. Soc. Jap. **1972**, *32*, 1565.
12. Hüller, A.; Physik, Z. **1974**, *270*, 343.
13. Vaks, V.G.; Schneider, V.E. Phys. Stat. Solidi (a) **1976**, *35*, 61.
14. Vlasova, A.A.; Tornau, E.E.; Schneider, V.E. Fiz. Tverd. Tela (Leningrad) **1978**, *20*, 858.
15. Yurtseven, H.; Salihoğlu, S.; Tüblek, A. Phase Trans. **1995**, *54*, 151.
16. Voronel, A.V.; Garber, S.R. Sov. Phys. JETP. **1967**, *25*, 970.
17. Fredericks, G.E. Phys. Rev. **1971**, *B4*, 911.
18. Schwartz, P. Phys. Rev. **1971**, *B4*, 920.
19. Wang, C.H. Wright, R.B. J. Chem. Phys. **1974**, *60*, 849.
20. Lushington, K.J.; Garland, C.W. J. Chem. Phys. **1980**, *72*, 5752.
21. Amitin, E.B.; Nabutovskaya, O.A. Sov. Phys. Solid State **1984**, *26*, 702.
22. Yamashita, H.; Uenishi, M.; Tatsuzaki, I. Solid State Comm. **1985**, *56*, 615.
23. Yurtseven, H.; Sherman, W.F. Phase Trans. **1995**, *54*, 1.
24. Seeck, O.H.; Hupfeld, D.; Krull, H.; Tolan, M.; Press, W. Phys. Rev. B Condens. Matt. **1998**, *58*, 623.
25. Yurtseven, H.; Kayişoğlu, D.; Sherman, W.F. Phase Trans. **1998**, *67*, 399.
26. Yurtseven, H.; Sherman, W.F. J. Mol. Struc. **1994**, *323*, 243.

Received November 24, 2000
Accepted December 10, 2000

Downloaded At: 03:12 30 January 2011

Request Permission or Order Reprints Instantly!

Interested in copying and sharing this article? In most cases, U.S. Copyright Law requires that you get permission from the article's rightsholder before using copyrighted content.

All information and materials found in this article, including but not limited to text, trademarks, patents, logos, graphics and images (the "Materials"), are the copyrighted works and other forms of intellectual property of Marcel Dekker, Inc., or its licensors. All rights not expressly granted are reserved.

Get permission to lawfully reproduce and distribute the Materials or order reprints quickly and painlessly. Simply click on the "Request Permission/Reprints Here" link below and follow the instructions. Visit the U.S. Copyright Office for information on Fair Use limitations of U.S. copyright law. Please refer to The Association of American Publishers' (AAP) website for guidelines on Fair Use in the Classroom.

The Materials are for your personal use only and cannot be reformatted, reposted, resold or distributed by electronic means or otherwise without permission from Marcel Dekker, Inc. Marcel Dekker, Inc. grants you the limited right to display the Materials only on your personal computer or personal wireless device, and to copy and download single copies of such Materials provided that any copyright, trademark or other notice appearing on such Materials is also retained by, displayed, copied or downloaded as part of the Materials and is not removed or obscured, and provided you do not edit, modify, alter or enhance the Materials. Please refer to our Website User Agreement for more details.

Order now!

Reprints of this article can also be ordered at
http://www.dekker.com/servlet/product/DOI/101081SL100002004